

DISCOVERY OF GRB 020405 AND ITS LATE RED BUMP

P. A. PRICE,^{1,2} S. R. KULKARNI,² E. BERGER,² D. W. FOX,² J. S. BLOOM,² S. G. DJORGOVSKI,² D. A. FRAIL,³ T. J. GALAMA,²
F. A. HARRISON,² P. MCCARTHY,⁴ D. E. REICHART,² R. SARI,⁵ S. A. YOST,² H. JERJEN,¹ K. FLINT,⁶ A. PHILLIPS,⁷
B. E. WARREN,¹ T. S. AXELROD,¹ R. A. CHEVALIER,⁸ J. HOLTZMAN,⁹ R. A. KIMBLE,¹⁰ B. P. SCHMIDT,¹
J. C. WHEELER,¹¹ F. FRONTERA,^{12,13} E. COSTA,¹² L. PIRO,¹² K. HURLEY,¹⁴ T. CLINE,¹⁵ C. GUIDORZI,¹³
E. MONTANARI,¹³ E. MAZETS,¹⁶ S. GOLENETSKII,¹⁶ I. MITROFANOV,¹⁷ D. ANFIMOV,¹⁷ A. KOZYREV,¹⁷
M. LITVAK,¹⁷ A. SANIN,¹⁷ W. BOYNTON,¹⁸ C. FELLOWS,¹⁸ K. HARSHMAN,¹⁸ C. SHINOHARA,¹⁸
A. GAL-YAM,¹⁹ E. OFEK,¹⁹ AND Y. LIPKIN¹⁹

Received 2002 July 31; accepted 2003 February 7

ABSTRACT

We present the discovery of GRB 020405 made with the Interplanetary Network (IPN). With a duration of 60 s, the burst appears to be a typical long-duration event. We observed the 75 arcmin² IPN error region with the Mount Stromlo Observatory's 50 inch robotic telescope and discovered a transient source that subsequently decayed and was also associated with a variable radio source. We identify this source as the afterglow of GRB 020405. Subsequent observations by other groups found varying polarized flux and established a redshift of 0.690 to the host galaxy. Motivated by the low redshift, we triggered observations with WFPC2 on board the *Hubble Space Telescope* (*HST*). Modeling the early ground-based data with a jet model, we find a clear red excess over the decaying optical light curves that is present between day 10 and day 141 (the last *HST* epoch). This bump has the spectral and temporal features expected of an underlying supernova (SN). In particular, the red color of the putative SN is similar to that of the SN associated with GRB 011121 at late time. Restricting the sample of GRBs to those with $z < 0.7$, a total of five bursts, red bumps at late times are found in GRB 970228, GRB 011121, and GRB 020405. It is possible that the simplest idea, namely, that all long-duration γ -ray bursts have underlying SNe with a modest dispersion in their properties (especially peak luminosity), is sufficient to explain the nondetections.

Subject heading: gamma rays: bursts

On-line material: color figures

1. INTRODUCTION

In recent years, several indirect lines of evidence have emerged connecting the class of long duration γ -ray bursts (GRBs) to massive stars. Every GRB afterglow with a sub-arcsecond position is associated with a star-forming galaxy (Bloom, Kulkarni, & Djorgovski 2002). Some of these galaxies are forming stars copiously with rates of a few hundred $M_{\odot} \text{ yr}^{-1}$ (Berger, Kulkarni, & Frail 2001; Frail et al. 2002). On smaller scales, some afterglows (the so-called dark bursts) show evidence for heavy dust extinction (Djorgovski et al. 2001; Piro et al. 2002). X-ray and optical

observations of some GRBs indicate substantial column densities (Owens et al. 1998; Galama & Wijers 2001). In addition, there is evidence for moderate circumburst densities, $n \sim 10 \text{ cm}^{-3}$, in some bursts (Harrison et al. 2001; Panaitescu & Kumar 2001; Yost et al. 2002). These indicators are consistent with GRBs originating in gas-rich star-forming regions (i.e., molecular clouds).

The most direct link between GRBs and massive stars comes from observations on stellar scales, namely, the detection of underlying supernovae (SNe) and X-ray spectral features. X-ray spectral features have been observed in a few GRBs (Piro et al. 2000; Reeves et al.

¹ Research School of Astronomy and Astrophysics, Mount Stromlo Observatory, via Cotter Road, Weston, ACT 2611, Australia.

² Palomar Observatory, 105-24, California Institute of Technology, Pasadena, CA 91125.

³ National Radio Astronomy Observatory, P.O. Box O, Socorro, NM 87801.

⁴ Carnegie Observatories, 813 Santa Barbara Street, Pasadena, CA 91101.

⁵ Theoretical Astrophysics, 130-33, California Institute of Technology, Pasadena, CA 91125.

⁶ UCO/Lick Observatory, Board of Studies in Astronomy and Astrophysics, University of California, 1156 High Street, Santa Cruz, CA 95064.

⁷ School of Physics, University of New South Wales, Sydney, NSW 2052, Australia.

⁸ Department of Astronomy, University of Virginia, P.O. Box 3818, Charlottesville, VA 22903-0818.

⁹ Department of Astronomy, MSC 4500, New Mexico State University, P.O. Box 30001, Las Cruces, NM 88003.

¹⁰ Laboratory for Astronomy and Solar Physics, NASA Goddard Space Flight Center, Code 681, Greenbelt, MD 20771.

¹¹ Astronomy Department, University of Texas, Austin, TX 78712.

¹² Istituto Astrofisica Spaziale e Fisica Cosmica, CNR, Area di Tor Vergata, Via Fosso del Cavaliere 100, 00133 Rome, Italy.

¹³ Dipartimento di Fisica, Università di Ferrara, Via Paradiso 12, 44100 Ferrara, Italy.

¹⁴ University of California, Space Sciences Laboratory, Berkeley, CA 94720.

¹⁵ NASA Goddard Space Flight Center, Code 661, Greenbelt, MD 20771.

¹⁶ Ioffe Physico-Technical Institute, Saint Petersburg 194021, Russia.

¹⁷ Space Research Institute, Profsojuznaya Str. 84/32, 117810 Moscow, Russia.

¹⁸ Department of Planetary Sciences, Lunar and Planetary Laboratory, Tucson, AZ 85721-0092.

¹⁹ School of Physics and Astronomy and Wise Observatory, Tel Aviv University, Tel Aviv 69978, Israel.

2002), although the detections generally have a low signal-to-noise ratio, and the interpretations are somewhat controversial. What is generally agreed, however, is that X-ray features would require the presence of high densities of iron on stellar scales.

The discovery of the unusual Type Ic SN 1998bw (Galama et al. 1998) in a nearby (~ 40 Mpc) galaxy within the small error box of GRB 980425 (Pian et al. 2000) suggested that at least some GRBs might be caused by SN explosions. Despite the fact that GRB 980425 was underenergetic compared to the cosmological GRBs (Frail et al. 2001) and may therefore represent an independent class of GRBs, the fact remains that SN 1998bw directly demonstrates that a massive star is capable of producing relativistic ejecta (Kulkarni et al. 1998)—an essential requirement for producing γ -rays.

The first indication of a SN underlying a cosmological GRB came from the observation of a red excess (“bump”) in the rapidly decaying afterglow of GRB 980326 (Bloom et al. 1999), which had a color and peak time consistent with SN 1998bw shifted to $z \sim 1$. However, the lack of a measured redshift for this GRB and the possibility of other explanations (e.g., dust echoes; Esin & Blandford 2000; Reichart 2001b) made the identification of the bump uncertain. Several attempts to identify similar bumps in the afterglows of GRBs with known redshift followed with mixed results: see Price et al. (2002) for a review.

These earlier results motivated us to successfully propose a large *Hubble Space Telescope* (*HST*) program to search for SNe underlying GRBs (GO-9180, P.I.: Kulkarni). *HST* is ideally suited to this effort since its stable point-spread function and high angular resolution make possible accurate and precise photometry of variable sources embedded on host galaxies. Low-redshift GRBs are particularly important to study since beyond a redshift of 1.2, the strong absorption in the SNe rest-frame spectra blueward of 4000 \AA covers the entire observed optical region, thus making searches all but impossible with current instruments.

To date, the best case for a SN underlying a cosmological GRB comes from *HST* observations of GRB 011121 ($z = 0.365$; Bloom et al. 2002; Garnavich et al. 2002). This is based on a bump in the optical afterglow light curves between 15 and 75 days, exhibiting a spectral turnover at $\sim 7200 \text{ \AA}$.

In addition, on the basis of early near-infrared and radio observations (Price et al. 2002), the afterglow of GRB 011121 exhibits clear evidence for a circumburst density $\rho \propto r^{-2}$ (where r is the radial distance from the burst). Such a density profile is indicative of stellar mass loss. Hence, from two independent lines of evidence, it can be inferred that the progenitor of GRB 011121 was a massive star.

However, not all GRBs have an underlying SN as bright as that of GRB 011121 (e.g., GRB 010921; Price et al. 2002). Thus, additional deeper searches for coincident SNe are necessary to determine whether the lack of an observed SN is due to dust obscuration, diversity in the brightness of SNe coincident with GRBs, or some subset of GRBs having a different progenitor.

So far, our discussion has been motivated by and based on observations. However, theorists have studied massive star models for long-duration GRBs for more than a decade. In particular, the collapsar model posits that GRBs arise when the cores of massive stars with sufficient angular momentum collapse and form black holes (Woosley 1993;

MacFadyen & Woosley 1999; MacFadyen, Woosley, & Heger 2001) whose accretion powers bursts of γ -rays. From the discussion in this section, it is clear that there is a good observational basis for the collapsar model. Detailed studies of the underlying SNe (or their absence) will provide much needed observational constraints to the collapsar model or other models that also require an associated SN event (e.g., supranova: Vietri & Stella 1998; cannonball: Dado, Dar, & De Rujula 2002). Here, we present the discovery of the afterglow of GRB 020405 and the subsequent search for and discovery with *HST* of a red bump in the afterglow that we suggest may be a SN underlying the GRB.

2. THE GRB AND ITS OPTICAL AFTERGLOW

On 2002 April 5 at 00:41:26 UT, the Interplanetary Network (IPN) consisting of *Ulysses*, *Mars Odyssey*/HEND, and *BeppoSAX* discovered and localized GRB 020405 (Hurley et al. 2002). With a duration of 60 s, the burst is a typical long-duration GRB (Fig. 1). The prompt emission can be well fitted by a Band function (Band et al. 1993) with the following parameters: low-energy spectral index $\alpha = -0.00 \pm 0.25$, high-energy spectral index $\beta = -1.87 \pm 0.23$, and break energy $E_b \sim 182 \pm 45 \text{ keV}$. The fluence, as measured by *Konus-WIND*, was $(7.40 \pm 0.07) \times 10^{-5} \text{ ergs cm}^{-2}$ (15–2000 keV), and the peak flux, averaged over 0.768 s, was $(5.0 \pm 0.2) \times 10^{-6} \text{ ergs cm}^{-2} \text{ s}^{-1}$.

We observed the 75 arcmin^2 error box of GRB 020405 with the robotic 50 inch telescope at Mount Stromlo Observatory (MSO) and the 40 inch telescope at Siding Spring Observatory (SSO), commencing approximately 17 hr after the GRB. From comparison of these images with images from the Digitized Sky Survey,²⁰ we were able to identify a bright ($R \sim 18.5 \text{ mag}$) source within the error box that was not present in the Sky Survey (Price, Schmidt, & Axelrod 2002). We undertook further imaging observations with the Wise 40 inch, SSO 2.3 m, and the Las Campanas du

²⁰ The Digitized Sky Surveys were produced at the Space Telescope Science Institute under U.S. Government grant NAG W-2166.

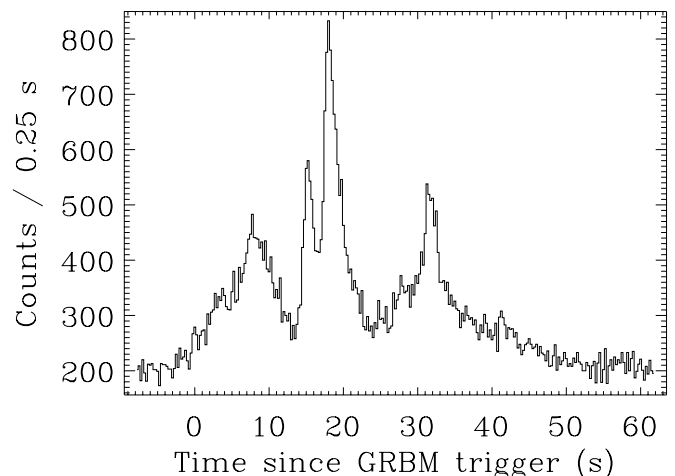


FIG. 1.—Time history of GRB 020405, as observed by *BeppoSAX* (40–700 keV).

Pont 100 inch telescopes (see Table 2) and found that the candidate faded.

In parallel, we undertook VLA observations of the source and found a 0.4 mJy radio counterpart (Berger, Kulkarni, & Frail 2002). The combination of a decaying optical source and a variable radio counterpart established that we had detected the afterglow of GRB 020405.

Several groups undertook follow-up observations of the optical afterglow. In particular, observations with the VLT rapidly identified the host galaxy to be a member of a group of interacting galaxies (Masetti et al. 2002a) at a redshift of $z = 0.695 \pm 0.005$ (Masetti et al. 2002b).

3. OPTICAL OBSERVATIONS OF THE AFTERGLOW AND THE HOST GALAXY

The low redshift of this event made it a prime candidate for a search for an underlying SN as a part of our large *HST* program. We staggered observations with the Wide Field Planetary Camera 2 (WFPC2) in F555W, F702W, and F814W between 19 and 31 days after the GRB in order to densely sample the peak of any underlying SN. We followed this sequence with observations in each filter approximately 2 months after the GRB in order to measure the SN decay. At each epoch, we exposed a total of 3900 s and used a 6 point dither pattern to recover the undersampled point-spread function.

We used “on-the-fly” preprocessing to produce de-biased, flattened images. The images were then drizzled (Fruchter & Hook 2002) onto an image with pixels smaller than the original by a factor of 0.5 using a *pixfrac* of 0.7.

Given that we had to tie the ground-based and *HST* data sets, we paid special attention to calibration. Calibration of field stars was performed through observation of Stetson standards²¹ with the Swope 40 inch telescope at LCO. We estimate that our calibration is accurate to approximately 0.05 mag. Images were bias-subtracted and flat-fielded in the standard manner and combined where necessary to increase the signal-to-noise ratio.

As can be seen from Figure 2, the host galaxy complex is quite bright ($R \sim 21$ mag). Hence, it is essential to employ image subtraction techniques on the ground-based images to obtain accurate light curves for the afterglow (Price et al. 2003; Bersier et al. 2003). We used the Novicki-Tonry photometry technique (see Price et al. 2002 for a description) on both the ground-based and *HST* observations to produce host-subtracted fluxes, under the assumption that the afterglow flux in the last available *HST* images in each filter were negligible (Tables 1 and 2). For the ground-based data, this is a reasonable assumption, since none of the observations are particularly deep, and the errors in the photometry will be larger than any offset. Similarly, for the F555W and F702W measurements with *HST*, which have late observations; but in F814W, there will be an uncertain, additional flux not included in our measurements since we are using subtracted fluxes. This additional flux is equal to the flux of the afterglow on June 9 in F814W, so it is important to bear in mind

²¹ Go to <http://cadwww.dao.nrc.ca/standards/>.

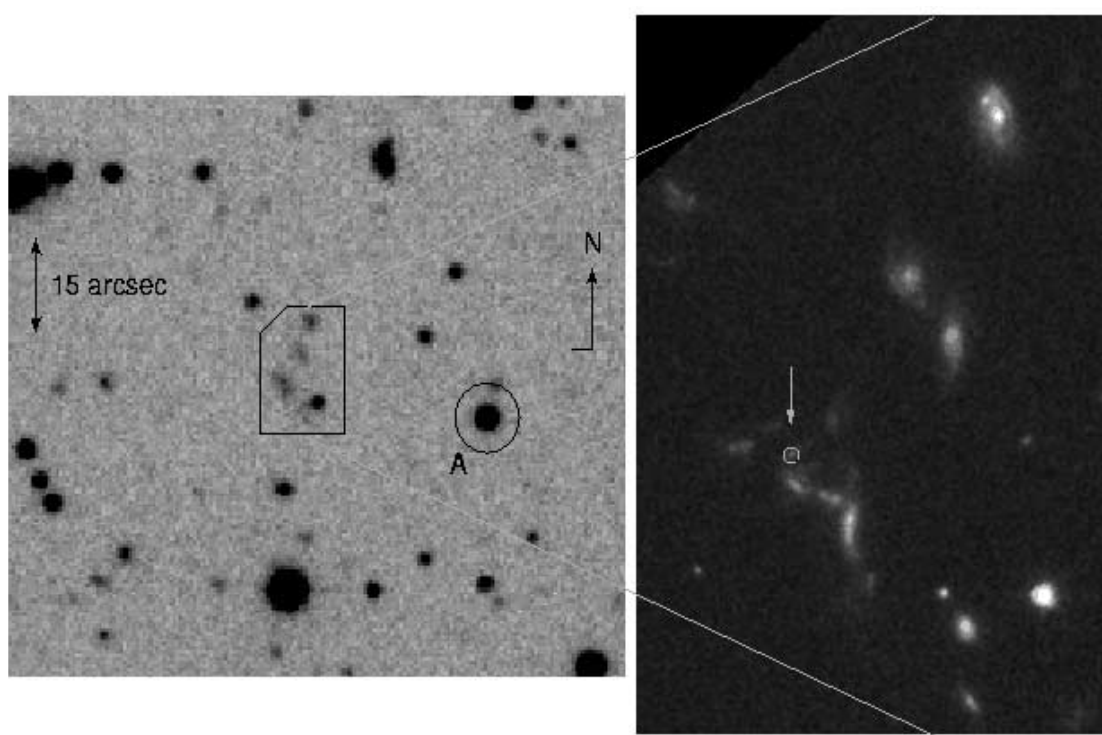


FIG. 2.—SSO 2.3 m (left) and *HST* (right) images of the host galaxy complex of GRB 020405. The GRB is $37^{\circ}10'$ east and $6^{\circ}69'$ north of the star marked A, for which we measure $B = 19.787 \pm 0.017$ mag, $V = 18.945 \pm 0.016$ mag, $R = 18.452 \pm 0.008$ mag, and $I = 17.980 \pm 0.010$ mag. The position of the GRB in the *HST* image is labeled. The host complex is relatively bright ($R \sim 21$ mag). [See the electronic edition of the *Journal* for a color version of this figure.]

TABLE 1
GROUND-BASED OBSERVATIONS OF THE AFTERGLOW
OF GRB 020405

Date (2002 April UT)	Filter	Flux (μ Jy)	Telescope
5.742	<i>B</i>	36 \pm 34	SSO40
6.506	<i>B</i>	8.5 \pm 1.1	SSO40
6.713	<i>B</i>	5.97 \pm 0.80	SSO40
7.367	<i>B</i>	4.6 \pm 1.2	dP
7.605	<i>B</i>	3.5 \pm 1.6	SSO40
5.752	<i>B_M</i>	29.5 \pm 3.7	MSO50
5.761	<i>B_M</i>	29.9 \pm 7.9	MSO50
5.772	<i>B_M</i>	30.1 \pm 2.5	MSO50
5.777	<i>B_M</i>	29.6 \pm 2.5	MSO50
5.781	<i>B_M</i>	28.5 \pm 2.6	MSO50
6.430	<i>B_M</i>	12.6 \pm 2.4	MSO50
9.434	<i>B_M</i>	3.0 \pm 1.9	MSO50
5.752	<i>R_M</i>	41.9 \pm 4.2	MSO50
5.761	<i>R_M</i>	42.4 \pm 4.4	MSO50
5.772	<i>R_M</i>	40.8 \pm 5.4	MSO50
5.777	<i>R_M</i>	41.5 \pm 3.5	MSO50
6.430	<i>R_M</i>	19.1 \pm 1.5	MSO50
9.434	<i>R_M</i>	5.3 \pm 2.8	MSO50
5.936	<i>R</i>	37.2 \pm 6.2	Wise40
11.694	<i>R</i>	1.5 \pm 1.1	SSO23
6.541	<i>I</i>	18.20 \pm 0.64	SSO40
6.750	<i>I</i>	15.39 \pm 0.63	SSO40
7.378	<i>I</i>	8.53 \pm 0.50	dP
7.639	<i>I</i>	4.9 \pm 5.4	SSO40

NOTE.—These data have been obtained by the Novicki-Tonry photometry technique, and hence contain no contribution from the host galaxy. Zero points were set through photometry of several calibrated field stars (sequence available upon request from pap@mso.anu.edu.au). These data have not been corrected for Galactic extinction. Telescopes are SSO40 (Siding Spring Observatory 40 inch), MSO50 (Mount Stromlo Observatory 50 inch robotic, using MACHO filters; Bessell & Germany 1999), dP (du Pont 100 inch at Las Campanas Observatory), Wise40 (Wise Observatory 40), and the SSO23 (Siding Spring Observatory 2.3 m).

that the F814W measurements presented below are an underestimate of the true flux for this filter only.

3.1. Host Galaxy Spectroscopy

We observed the afterglow and host galaxy of GRB 020405 with the Echellette Spectrograph and Imager (Sheinis et al. 2002) on Keck II at 2002 April 8.41 UT in poor seeing conditions. We used a $0''.75$ wide slit close to the parallactic angle and obtained two 1800 s exposures in echellette mode with a small dither on the slit. We used custom software to straighten the echelle orders before combining the individual exposures and extracting the spectrum using IRAF. Arc lamp exposures were used for wavelength calibration, with a resultant scatter of 0.06 Å. An observation of Feige 34 was used for flux calibration. An earlier spectrum was also obtained from the Baade Telescope but with lower resolution and signal-to-noise ratio.

We detect several bright emission lines that we attribute to [O II], H β , and [O III] at a mean heliocentric redshift of 0.68986 ± 0.00004 , consistent with the measurement first reported by Masetti et al. (2002b). We list these emission lines in Table 3. Using the observed [O II] and H β line fluxes and assuming a flat lambda cosmology with $H_0 = 65 \text{ km s}^{-1}$

TABLE 2
HST OBSERVATIONS OF THE AFTERGLOW OF
GRB 020405

Date (2002 UT)	Filter	Flux (μ Jy)
24.225 Apr	F555W	0.269 \pm 0.012
5.585 May	F555W	0.112 \pm 0.012
2.636 Jun	F555W	0.047 \pm 0.011
23.171 Aug	F555W	...
28.388 Apr	F702W	0.544 \pm 0.010
1.574 May	F702W	0.370 \pm 0.010
3.579 May	F702W	0.333 \pm 0.009
1.568 Jun	F702W	0.091 \pm 0.009
23.374 Aug	F702W	...
26.229 Apr	F814W	1.078 \pm 0.018
1.440 May	F814W	0.756 \pm 0.018
9.513 Jun	F814W	...

NOTE.—These data were obtained through Novicki-Tonry photometry and hence contain no contribution from the host galaxy. Those measurements for which no flux is recorded are the last available images in each filter: the flux of the afterglow is assumed to be zero in each of these for the purposes of Novicki-Tonry photometry. Counts were converted to fluxes by using IRAF/SYNPHOT to calculate the response to a constant flux of 1 mJy. The resultant fluxes are hence analogous to AB magnitudes. These measurements have been corrected for charge transfer (in-)efficiency (CTE) using the prescription of Dolphin 2000.

Mpc $^{-1}$ and $\Omega_M = 0.3$, we calculate (Kennicutt 1998) a star formation rate of $4 M_\odot \text{ yr}^{-1}$. This star formation rate is uncorrected for extinction or stellar absorption and is therefore a lower limit.

4. MODELING THE AFTERGLOW

We model the light curves (Fig. 3) by adopting a standard afterglow model with power-law temporal decay and a power-law spectrum, $F_\nu \propto t^{\alpha} \nu^{\beta}$. Due to the bright host galaxy complex, we include in our data set only those values in the literature that have been derived from

TABLE 3
LINES IDENTIFIED IN THE SPECTRUM OF THE HOST GALAXY OF GRB 020405

λ_{obs} (Å)	Line	F_{obs}	EW (Å)	GW (Å)
6298.67 \pm 0.10	[O II]	55.7 \pm 4.7	28.0 \pm 4.7	2.08 \pm 0.22
6303.59 \pm 0.04	[O II]	64.5 \pm 3.7	31.8 \pm 4.6	1.28 \pm 0.09
6539.7	[Ne III]	13.1 \pm 5.1	7.0 \pm 3.0	2.2
7337.13 \pm 0.24	H γ	19.9 \pm 5.3	11.6 \pm 3.9	1.88 \pm 0.60
8217.42 \pm 0.11	H β	66.3 \pm 5.7	54 \pm 11	2.54 \pm 0.24
8382.25 \pm 0.08	[O III]	51.1 \pm 3.9	26.3 \pm 5.3	2.29 \pm 0.17
8463.42 \pm 0.02	[O III]	201.9 \pm 3.7	71.7 \pm 5.9	2.545 \pm 0.052

NOTE.—Left to right: Columns are the observed wavelength of the line, line identification, observed flux corrected for Galactic extinction using $E_{(B-V)} = 0.054$ in units of $10^{-18} \text{ ergs cm}^{-2} \text{ s}^{-1}$, observed equivalent width (uncorrected for contamination by the afterglow), and observed Gaussian width. The line at $\lambda 6303.59$ is affected by a bright night sky line. Given the suggestion that GRB host galaxies may exhibit strong [Ne III] emission (Bloom, Djorgovski, & Kulkarni 2001), we have included an entry for this line.

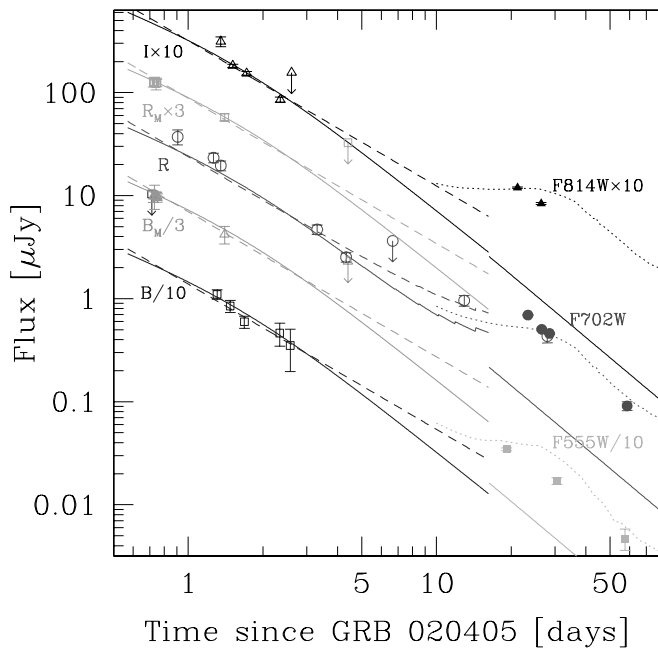


FIG. 3.—Light curves of the optical afterglow of GRB 020405, assuming zero afterglow flux in the final *HST* measurements. *Open symbols*: Ground-based measurements. *Filled symbols*: *HST* measurements. *Dashed line*: Single power-law decay model (isotropic emission). *Solid line*: Broken power-law decay model (jet). Both models incorporate a power-law spectrum and are fitted to data taken before 10 days. We have plotted the light curve of SN 1998bw shifted to $z = 0.690$ and dimmed by 0.5 mag over the *HST* data for a rough comparison. The flux in the F814W filter is an underestimate: see the text for an explanation. Reddening the SN 1998bw light curve to account for host extinction may produce a better match, but the extinction along the line of sight cannot be precisely determined from the current data. [See the electronic edition of the *Journal* for a color version of this figure.]

host-subtracted images; specifically, the measurements of Bersier et al. (2003; corrected for the apparent difference in reference star magnitudes) and those presented here. In the first round of analysis, we restrict ourselves to data taken prior to 10 days after the GRB. We obtain a fairly poor fit with $\chi^2/\text{dof} = 53.4/29$, $\alpha = -1.41$, and $\beta = -1.25$. We notice that the model slightly overpredicts the flux for the earliest data from the MSO 50 inch telescope. This may suggest the presence of a jet break about 1 day after the GRB.

Bersier et al. (2003) have detected strong polarization of the afterglow emission (9.9%) at 1.3 days after the GRB, which then appears to have declined to about 1.9% by 2.1 days after the GRB (Covino et al. 2002). Sari (1999) predicted the polarization of GRB afterglows to peak at about 10% at the time of the jet break for GRBs that are not viewed far off-axis. The behavior of the polarization curve, therefore, also argues for the presence of a jet break about a day after the GRB. The low radio flux (E. Berger et al. 2003, in preparation) compared to the bright optical afterglow may also be evidence of an early jet break.

We therefore adopt a broken power-law temporal decay with indices α_1 (early times), α_2 (late times), and a jet break time (t_{jet}). The power-law indices are functions of the electron energy distribution index, p [$N(\gamma) \propto \gamma^{-p}$ for $\gamma > \gamma_{\text{min}}$]. However, given the sparse data, we make the ad hoc simplifying assumption that the optical band is above the cooling frequency and the circumburst medium is homogenous. In

this case, $\alpha_1 = (3p - 2)/4$ and $\alpha_2 = -p$ (Sari, Piran, & Halpern 1999).

With these assumptions, we obtain a much-improved fit, $\chi^2/\text{dof} = 35.9/28$: $p = 1.93 \pm 0.25$ and $t_{\text{jet}} = 1.67 \pm 0.52$ days. Adding a systematic error of 0.06 mag in quadrature with the measurement errors to account for differences between data taken with different instruments reduces the χ^2 to match the degrees of freedom. In our experience, this is an expected level of systematic error.

The redshift of GRB 020405, $z = 0.690$, and the observed spectrum of the burst, imply an isotropic equivalent k -corrected (Bloom, Frail, & Sari 2001) energy release, $E_{\text{iso}}(\gamma)(20\text{--}2000 \text{ keV}) = (7.37 \pm 0.80) \times 10^{52}$ ergs. The k -correction ($k = 1.31 \pm 0.09$) is small and rather precise, given the spectral constraints from *BeppoSAX*. From our best-fit value of t_{jet} , using the specific formulation of Frail et al. (2001), we calculate a jet opening angle of $(5.83 \pm 0.69) n^{1/8}$ deg, where n is the number density of the ambient medium in units of cm^{-3} . The beaming-corrected energy is thus $E_{\gamma} = (3.82 \pm 0.94) \times 10^{50} n^{1/4}$ ergs, at the low end of (but consistent with) the distribution centered on $9 \times 10^{50} n^{1/4}$ ergs for long-duration GRBs (Frail et al. 2001).

We can also measure the dust extinction from the afterglow data by demanding that the intrinsic spectral slope match that predicted by a particular theoretical model (dependent on the density profile and the location of the cooling frequency relative to the optical bands) and attributing any observed reddening to extinction (see, e.g., Price et al. 2002). Assuming an SMC extinction curve (Reichart 2001a), we measure the extinction to be $0.22 \text{ mag} < A_V^{\text{host}} < 0.64 \text{ mag}$, depending on the choice of afterglow model.

4.1. Late-Time Data: A Red Bump

We now turn our attention to data taken after 10 days from the GRB. We note that there is a strong excess in each of the three *HST* filters. This excess (“bump”) exists independent of the assumed geometry of the afterglow but is more pronounced for a jet model (discussed above). We suggest that this excess may be due to a SN that exploded within about a week of the GRB. Although it is not possible to analyze the bump in detail (in particular, its flux relative to SN 1998bw) until later *HST* observations have been made of the host galaxy to remove the assumption of zero afterglow flux in the last available epochs, we can make a number of qualitative statements.

First, the peak of the bump is not well constrained by these data and appears to be between 10 and 25 days after the GRB.

Second, fitting a power-law spectrum, $F_{\nu} \propto \nu^{\beta}$, to the *HST* data demonstrates that the bump is quite red, with $\beta = -3.98 \pm 0.18$ (i.e., $B-V = 1.07 \text{ mag}$, $V-R = 0.90 \text{ mag}$), in contrast to $\beta = -1.23 \pm 0.12$ measured for the afterglow at early times—further evidence for the existence of two components. This measurement of the spectral index is similar to that for the SN underlying GRB 011121, which has $\beta \approx -3.5$ between the F450W and F555W filters at late time (Bloom et al. 2002). However, the SN underlying GRB 011121 appeared somewhat bluer in the F555W filter than SN 1998bw (Garnavich et al. 2002), while GRB 020405’s red bump appears more red. For GRB 011121, the SN spectral peak was at $\sim 7500 \text{ \AA}$ (Bloom et al. 2002), which corresponds to 9300 \AA at the redshift of GRB 020405. Since

the spectrum is well described by a single power law, the spectral peak of a SN would be redward of 8700 Å, which is consistent with the data on GRB 011121. Thus, the broadband spectra of the red bump appears to be grossly similar to that of GRB 011121 upon first inspection. Some differences in color are not unexpected due to the uncertain extinction along the line of sight to GRB 020405 and the expected diversity in the properties (e.g., jets) of these energetic SNe.

5. CONCLUSIONS

Here we report the discovery of the nearby ($z \sim 0.7$) GRB 020405 and the subsequent discovery of the afterglow. The GRB itself, with a duration of 60 s, appears to be a typical long-duration burst. The optical afterglow data, spanning about 10 days, can be fitted with a standard broken power law with a break time of about 1.5 days. Identifying this break with a jet, we obtain a beaming-corrected energy release of about 4×10^{50} ergs, typical of that inferred for long-duration GRBs.

Motivated by the low redshift, we undertook multicolor observations of the afterglow with *HST*. We found an excess over the flux predicted by the modeling of the afterglow from ground-based data. The overall broadband spectrum of the bump as well as its temporal evolution are most simply explained as due to an underlying SN that exploded at about the same time as the GRB.

In Price et al. (2003), we summarize the searches for underlying SNe in $z < 1.2$ GRBs (the redshift restriction arising from the fact that the searches are conducted in the optical band: see § 1). Including GRB 020405, there are 13 GRBs with $z < 1.2$. A strong case for an underlying SN can be made for GRB 011121 ($z = 0.365$; Bloom et al. 2002; Garnavich et al. 2002) and GRB 020405 ($z = 0.690$). A good case can be made for GRB 970228 ($z = 0.695$; Reichart 1999; Galama et al. 2000) and GRB 980326 (z unknown; Bloom et al. 1999). At first blush, this appears to be a low yield and suggestive that there is diversity either in the

progenitors of long-duration GRBs or in the properties of underlying SNe, or both.

However, it is important to bear in mind that one of the two unique signatures for a SN is the spectral rollover at short wavelengths, namely, below about 4000 Å (see Bloom et al. 1999). Thus, for $z \sim 1$, observations in the *R* and *I* bands are critical, whereas at lower redshifts, observations in *V* and *R* bands are critical. The *I* band is quite noisy for ground-based observations, whereas most afterglows are well observed in *R* and *V* bands.

Restricting to $z < 0.7$, we find five GRBs (970228, 011121, 020405, 990712, and 010921), of which underlying SNe have been identified in the first three and possibly in GRB 990712 (Björnsson et al. 2001). The limit for an underlying SN in GRB 010921 is not very stringent (Price et al. 2002); in particular, an underlying SN fainter by more than 2 mag relative to that of SN 1998bw (about as bright as typical SNe Ib/c) would have escaped identification. It is thus premature to conclude that we need several progenitors to cause GRBs. What we can conclude, though, is that dense sampling in several bands of nearby GRBs is likely to remain a productive activity.

B. P. S. and P. A. P. thank the ARC for supporting Australian GRB research. GRB research at Caltech (S. R. K., S. G. D., F. A. H., R. S.) is supported by grants from NSF and NASA. K. H. is grateful for *Ulysses* and IPN support under JPL contract 958056 and NASA grant NAG5-11451. Support for Proposal *HST*-GO-09180.01-A was provided by NASA through a grant from the Space Telescope Science Institute, which is operated by the Association of Universities for Research in Astronomy, Inc., under NASA contract NAS5-26555. We thank M. Pettini, N. Reddy, and C. Steidel for undertaking observations at Keck under the auspices of the Caltech ToO program. Finally, we thank the staff of MSO, SSO, Wise, LCO, Keck, and the STScI for their assistance.

REFERENCES

- Band, D., et al. 1993, *ApJ*, 413, 281
 Berger, E., Kulkarni, S. R., & Frail, D. A. 2001, *ApJ*, 560, 652
 ———. 2002, *GCN Circ.*, 1331, 1 (<http://gcn.gsfc.nasa.gov/gcn/gcn3/1331.gcn3>)
 Bersier, D., et al. 2003, *ApJ*, 583, L63
 Bessell, M. S., & Germany, L. M. 1999, *PASP*, 111, 1421
 Björnsson, G., Hjorth, J., Jakobsson, P., Christensen, L., & Holland, S. 2001, *ApJ*, 552, L121
 Bloom, J. S., Djorgovski, S. G., & Kulkarni, S. R. 2001, *ApJ*, 554, 678
 Bloom, J. S., Frail, D. A., & Sari, R. 2001, *AJ*, 121, 2879
 Bloom, J. S., Kulkarni, S. R., & Djorgovski, S. G. 2002, *AJ*, 123, 1111
 Bloom, J. S., et al. 1999, *Nature*, 401, 453
 ———. 2002, *ApJ*, 572, L45
 Covino, S., et al. 2002, *GCN Circ.*, 1431, 1 (<http://gcn.gsfc.nasa.gov/gcn/gcn3/1431.gcn3>)
 Dado, S., Dar, A., & De Rujula, A. 2002, *A&A*, 388, 1079
 Djorgovski, S. G., Frail, D. A., Kulkarni, S. R., Bloom, J. S., Odewahn, S. C., & Diercks, A. 2001, *ApJ*, 562, 654
 Dolphin, A. E. 2000, *PASP*, 112, 1397
 Esin, A. A., & Blandford, R. 2000, *ApJ*, 534, L151
 Frail, D. A., et al. 2001, *ApJ*, 562, L55
 ———. 2002, *ApJ*, 565, 829
 Fruchter, A. S., & Hook, R. N. 2002, *PASP*, 114, 144
 Galama, T. J., & Wijers, R. A. M. J. 2001, *ApJ*, 549, L209
 Galama, T. J., et al. 1998, *Nature*, 395, 670
 ———. 2000, *ApJ*, 536, 185
 Garnavich, P. M., et al. 2002, *ApJ*, submitted (astro-ph/0204234)
 Harrison, F. A., et al. 2001, *ApJ*, 559, 123
 Hurley, K., et al. 2002, *GCN Circ.*, 1325, 1 (<http://gcn.gsfc.nasa.gov/gcn/gcn3/1325.gcn3>)
 Kennicutt, R. C. 1998, *ARA&A*, 36, 189
 Kulkarni, S. R., et al. 1998, *Nature*, 395, 663
 MacFadyen, A. I., & Woosley, S. E. 1999, *ApJ*, 524, 262
 MacFadyen, A. I., Woosley, S. E., & Heger, A. 2001, *ApJ*, 550, 410
 Masetti, N., et al. 2002a, *GCN Circ.*, 1375, 1 (<http://gcn.gsfc.nasa.gov/gcn/gcn3/1375.gcn3>)
 ———. 2002b, *GCN Circ.*, 1330, 1 (<http://gcn.gsfc.nasa.gov/gcn/gcn3/1330.gcn3>)
 Owens, A., et al. 1998, *A&A*, 339, L37
 Panaitescu, A., & Kumar, P. 2001, *ApJ*, 560, L49
 Pian, E., et al. 2000, *ApJ*, 536, 778
 Piro, L., et al. 2000, *Science*, 290, 955
 ———. 2002, *ApJ*, 577, 680
 Price, P. A., Schmidt, B. P., & Axelrod, T. S. 2002, *GCN Circ.*, 1326, 1 (<http://gcn.gsfc.nasa.gov/gcn/gcn3/1326.gcn3>)
 Price, P. A., et al. 2002, *ApJ*, 572, L51
 ———. 2003, *ApJ*, 584, 941
 Reeves, J. N., et al. 2002, *Nature*, 416, 512
 Reichart, D. E. 1999, *ApJ*, 521, L111
 ———. 2001a, *ApJ*, 553, 235
 ———. 2001b, *ApJ*, 554, 643
 Sari, R. 1999, *ApJ*, 524, L43
 Sari, R., Piran, T., & Halpern, J. P. 1999, *ApJ*, 519, L17
 Sheinis, A., Bolte, M., Epps, H., Kibrick, R., Miller, J., Radovan, M., Bigelow, B., & Sutin, B. 2002, *PASP*, 114, 851
 Vietri, M., & Stella, L. 1998, *ApJ*, 507, L45
 Woosley, S. E. 1993, *ApJ*, 405, 273
 Yost, S. A., et al. 2002, *ApJ*, 577, 155